Railway Engineering Science
https://doi.org/10.1007/s40534-023-00321-5

A discussion about the limitations of the Eurocode's high-speed load model for railway bridges

Gonçalo Ferreira[1] · Pedro Montenegro[1] · José Rui Pinto[1] · António Abel Henriques[2] · Rui Calçada[1]

Received: 9 December 2022 / Revised: 17 August 2023 / Accepted: 21 September 2023

Abstract
High-speed railway bridges are subjected to normative limitations concerning maximum permissible deck accelerations. For the design of these structures, the European norm EN 1991-2 introduces the high-speed load model (HSLM)—a set of point loads intended to include the effects of existing high-speed trains. Yet, the evolution of current trains and the recent development of new load models motivate a discussion regarding the limits of validity of the HSLM. For this study, a large number of randomly generated load models of articulated, conventional, and regular trains are tested and compared with the envelope of HSLM effects. For each type of train, two sets of 100,000 load models are considered: one abiding by the limits of the EN 1991-2 and another considering wider limits. This comparison is achieved using both a bridge-independent metric (train signatures) and dynamic analyses on a case study bridge (the Canelas bridge of the Portuguese Railway Network). For the latter, a methodology to decrease the computational cost of moving loads analysis is introduced. Results show that some theoretical load models constructed within the stipulated limits of the norm can lead to effects not covered by the HSLM. This is especially noted in conventional trains, where there is a relation with larger distances between centres of adjacent vehicle bogies.

Keywords High-speed load model · Dynamic analysis · High-speed railways · Train signature · Railway bridges · Deck acceleration

1 Introduction

The evaluation of running safety on bridges has been a widely studied topic in the last years [1–3]. In particular, the design of high-speed railway bridges must fulfil, among others, several safety and serviceability normative criteria related to the dynamic behaviour of the structure under railway traffic. Among those criteria, particular attention should be given to the one related to the maximum deck accelerations specified in the European norm EN 1990-Annex A2 [4], since it often conditions the bridge design. This criterion stipulates a maximum deck acceleration of 3.5 and 5.0 m/s^2 for bridges with ballasted and non-ballasted tracks, respectively. While the former comes from the test rig experiments described in [5, 6], in which it was concluded that for accelerations above 0.7g the ballast layer loses its interlocking capabilities, leading to the instability of the ballast track and consequent higher probability of derailment, the latter is related to the fact that for accelerations above 1g there is a higher risk of uplift effects of bearings and train wheels. Then, according to the recommendation proposed by Ref. [7], a safety factor of 2 is applied to these values, leading to the above-mentioned limits stipulated by the norm.

To generalize the design of railway bridges subjected to important dynamic effects caused by the train passages, usually those designed for speeds greater than 200 km/h, the European Commission's regulation on the Technical Specifications for Interoperability [8] stated that these structures must be checked through the high-speed load model (HSLM)

✉ Gonçalo Ferreira
goncalo.ferreira@fe.up.pt

Pedro Montenegro
paires@fe.up.pt

António Abel Henriques
aarh@fe.up.pt

Rui Calçada
ruiabc@fe.up.pt

[1] CONSTRUCT-LESE, Faculty of Engineering, University of Porto, Rua Dr. Roberto Frias, 4200-465 Porto, Portugal

[2] CONSTRUCT-LABEST, Faculty of Engineering, University of Porto, Rua Dr. Roberto Frias, 4200-465 Porto, Portugal

Published online: 28 February 2024

specified in the European norm EN 1991-2 [9]. This load model, which dated from 1999 and was proposed in Ref. [10], was built based on the idea of separating the dynamic response of the train from the response of the bridge to facilitate the comparison of the dynamic loading effects caused by different trains. Such separation led to the definition of a train spectrum, called train signature, which was successfully obtained through a method called decomposition of the excitation at resonance (DER method). However, many other authors continue to contribute to the development of this type of train spectra for analysing the structural response under railway traffic. Vestroni and Vidoli [11] developed an approach based on a non-dimensional representation of the bridge response and Fourier transform of the train loads. Matsuoka et al. [12] defined the train spectrum of the Italian ETR-1000 train to study the influence of local deck vibrations on the assessment of the maximum accelerations in a steel–composite high-speed railway bridge. Auersch [13] studied resonant effects in railway bridges using modal force excitation techniques and train axle sequence spectra.

The first approach for defining an all-encompassing load model to be adopted by the norms, however, was not the HSLM, but the UNIV-A model, also developed by the ERRI committee. This load model took the properties of the Eurostar articulated train as a basis, with an individual axle load of 170 kN, and considered a variation of the coach length between 18 and 27 m [14]. The objective was to guarantee that the signature envelope of this model could cover the effects caused by both articulated (Eurostar and Thalys 2) and conventional (ICE2 and ETR) trains. However, this model proved to be insufficient to cover the effects of the Virgin and Talgo trains, namely for the excitation wavelengths λ of 24 m for the former and between 12.5 and 14.0 m for the latter. Such drawback led to the development of the current HSLM, composed of two sets of models, namely the HSLM-A, which consists of 10 load schemes to be used in the design of continuous bridges or simply supported structures with spans greater than 7 m, and the HSLM-B, which comprises a series of equally spaced 170 kN point forces to be used in the design of simply supported bridges with spans less than 7 m.

Although the HSLM continues to be the most complete load model currently existing, its limits of validity have been recently discussed by some authors. Based on such discussion, the following research questions may arise:

1. Is the current HSLM suited to represent future (and existing) trains that do not necessarily respect its limits?
2. How well do the 10 HSLM-A train configurations cover the dynamic effects of all possible articulated, conventional and regular trains that they are meant to do?
3. Does the lack of definition of some HSLM limiting parameters, such as the distance between the centres of bogies between adjacent vehicles d_{BS} in conventional trains, affect the evaluation of these same limits?

The first question is related to the fact that the current limits of validity of the HSLM defined in Annex E of EN 1991-2 [9] (hereinafter referred to as Annex E) are not broad enough to cover new and future trains. An example of such limitation is the recent introduction into service of the German high-speed train ICE4 with a coach length D of 28.75 m [15], which has been reported to cause acceleration responses on railway bridges that are not covered by the HSLM envelope: Reiterer et al. [16] observed that the ICE4 can produce vertical deck acceleration more than double than the HSLM-A. This problem is currently leading to new proposals for load models for railway dynamic analysis, in which two international consortia, one from the European Project In2Track3 [17] and another from the German Federal Railway Authority [18, 19], stand out. Both works are focused on the definition of alternative load models that may cover the effects of recent and future trains characterized by design parameters outside the ranges of variations of the current HSLM, but that were adopted by vehicle manufactures due to competition and economic reasons. In both approaches, the authors assess the train signature envelopes, as well as bridge responses obtained with dynamic numerical finite element (FE) analysis. Regarding the latter, Vorwagner et al. [19] reported that their study covers a wide range of train configurations and bridge characteristics, totalling around more than 17 million dynamic analyses. Such scale brings with it concerns about the computational cost associated with performing dynamic analysis on FE models. Envisaging the possibility of train manufacturers designing new high-speed trains that do not fully meet the geometric limits stipulated by Annex E due to economic reasons (avoiding short length coaches, for example), Unterweger et al. [20] investigated the most critical parameters that need to be fulfilled to ensure that the new vehicle is in line with the HSLM. The authors performed a study with eight fictitious trains characterized by limit values specified in Annex E, or slightly outside those limits ($D = 16$ m, $D = 28.5$ m, the spacing of axles within a bogie $d_{BA} = 1.5$, and $d_{BA} = 5.4$), to assess which properties most contribute to larger responses in a set of single-span railway bridges. They proposed a methodology to identify the most critical bridges, in terms of length and first natural frequency, to reduce the number of bridges that must be investigated with the introduction in the network of new and more aggressive trains, and concluded that, from all train parameters ranges stipulated by Annex E, only a few are critical for

the bridge response, mainly the distance d_{BA}, for which a small variation in its value may strongly affect the resonance phenomena.

Although the lack of coverage of the HSLM regarding new trains is already being studied by the scientific community, the studies related to the two remaining questions are still scarce in literature. Museros et al. [21] assessed the effects caused by articulated trains that fulfil the validity limits of the HSLM stipulated by the Annex E. They concluded that the limitation that defines the ratio between the coach length D over the axle spacing within a bogie d_{BA} should be close to an integer value is not important, while only very few cases of articulated trains defined within the premises of Annex E would lead to an exceedance in the vertical acceleration limits. However, the limits of validity regarding conventional or regular trains were outside the scope of this work and, since only articulated trains were studied, no conclusions regarding the lack of information about the d_{BS} distance were drawn.

While some attention is given in the present work to the issues raised in the first aforementioned question, by systematically checking how the HSLM covers, or not, the effects caused by trains defined within a wider parameter interval than that defined in the norm [9], the main focus and novelty of this article are more concentrated on answering the other two questions. Regarding the second one, the effects caused by a vast set of randomly generated train load models with properties within the limits specified in Annex E, both articulated, conventional and regular, are compared with those caused by the HSLM. Such comparison is performed both in terms of analytical signature envelopes of both sets, as well as with a complete numerical dynamic analysis carried out in a specific case study bridge to explicitly compute its maximum acceleration response and compare it with the HSLM acceleration envelopes. To increase the computational efficiency, an optimized method to perform moving load dynamic analyses is also proposed in this regard. Moreover, the lack of definition regarding some geometrical parameters in Annex E raised in the third question, especially the distance d_{BS} in conventional trains, is also addressed in this work to analyse how this issue may affect the validity of the HSLM.

It is therefore clear that the answers to the second and third questions raised above remain barely explored in the literature, which represents a gap of knowledge in this particular field. Hence, the findings obtained from this study aim to contribute to the identification of the main limitations of the current load models used to design high-speed railway bridges, as well as to open new research paths to improve these models, particularly by proposing a simplified methodology that can expedite dynamic calculations on different sets of wavelengths. The article is structured in five sections, in which the methodology to compare the HSLM effects with those caused by the theoretical trains randomly generated through the procedure stipulated in Annex E is presented in Sect. 2, while the numerical models used in this work are described in Sect. 3. Section 4 is dedicated to the results obtained in the preliminary analysis performed with the train signature technique and in the complete dynamic analysis carried out with the case study bridge. Finally, in Sect. 5, the main conclusions from this work are summarized and recommendations for future work are proposed.

2 Methods for dynamic assessment

The present section goes over the methodologies employed in this study, starting with an overview of the concept of train signatures and proceeding to introduce a procedure used for speeding up the process of dynamic analysis. At the end, an explanation of the numerical work can be found.

2.1 Train signatures

The decomposition of excitation at resonance (DER) method was introduced in Ref. [10] and applies to simple spans, under the following conditions:

- Inertial interaction is ignored.
- Only the first vibration mode is considered.
- The response is decomposed into a Fourier series, retaining only the resonance term.
- The results are independent of time.

Using this method, the maximum mid-span acceleration $\ddot{y}$ can be given as a product of a constant factor C_t, a function for the influence line $A(\cdot)$ and the train spectrum $G(\cdot)$:

$$\ddot{y} \leq C_t A\left(\frac{L}{\lambda}\right) G(\lambda). \tag{1}$$

For a bridge with a first frequency f_0, generalized stiffness K, span L and linear mass m, the constant factor is given by

$$C_t = \frac{8\pi f_0^2}{K} = \frac{4}{mL\pi}. \tag{2}$$

Given the excitation wavelength λ, the influence line function is taken as

$$A\left(\frac{L}{\lambda}\right) = \left| \frac{\cos\left(\frac{\pi L}{\lambda}\right)}{\left(\frac{2L}{\lambda}\right)^2 - 1} \right|. \tag{3}$$

Regarding the train, with N loads P_k at coordinates x_k at position k, on a bridge with damping ratio ξ, its spectrum is given by

$$G(\lambda) \cong \underset{i=1,\, N-1}{\text{MAX}} \frac{1}{\xi x_i} \left[\sqrt{\left(\sum_{k=0}^{i} P_k \cos\left(\frac{2\pi x_k}{\lambda}\right) \right)^2 + \left(\sum_{k=0}^{i} P_k \sin\left(\frac{2\pi x_k}{\lambda}\right) \right)^2} \left(1 - \mathrm{e}^{-2\pi\xi\frac{x_i}{\lambda}}\right) \right]. \tag{4}$$

The DER method is sensitive to some of its errors, namely due to:

- High wavelengths and short trains influence on the resonance criteria.
- Values of zero of the influence line.
- Overestimation of the response for high damping coefficients.

Nonetheless, the method can also be used to approximate the maximum mid-span displacement y, given the first angular frequency ω_0 and the static displacement given by the train loads y_{stat}, as

$$y \cong y_{\text{stat}} + \frac{\ddot{y}_{\max}}{\omega_0^2}. \tag{5}$$

One major aspect of the application of this methodology is that it introduces the concept of train signature. Since the train spectrum does not allow a separate assessment of the train effect from the bridge response, given its dependence on the damping coefficient, the train signature $S_0(\lambda)$ is the result of

$$S_0(\lambda) = \lim_{\xi \to 0} G(\lambda), \tag{6}$$

and as such

$$S_0(\lambda) = \underset{i=1,\, N-1}{\text{MAX}} \frac{1}{\xi x_i} \left[\sqrt{\left(\sum_{k=0}^{i} P_k \cos\left(\frac{2\pi x_k}{\lambda}\right) \right)^2 + \left(\sum_{k=0}^{i} P_k \sin\left(\frac{2\pi x_k}{\lambda}\right) \right)^2} \right]. \tag{7}$$

These signatures allow for fast comparisons between the different train effects. Knowing the signatures of the trains in operation on a given line, a new train can be deemed as either apt or inapt for running on that line, by simply comparing the new vehicle signature to the previous ones.

2.2 Single load linear superposition (SLSS)

The fulfilment of the present study objectives is dependent on the ability to perform several thousand dynamic analyses in varying scenarios. Whether considering the random variation of a train geometrical configuration or the randomness of bridge characteristics, there are advantages in simplifying the dynamic analysis process. In the scope of this work, the metric being evaluated in ballasted bridges is the vertical deck acceleration, and therefore dynamic analyses with moving loads are sufficient. In this approach, different train models are described as a series of individual axle loads and the distances between them—e.g. how the HSLM is represented. Generally, the first step in such an analysis is to determine the individual nodal loads, for each axle load and rail node. Instead, the proposed procedure (SLLS) considers the dynamic effects caused by a single moving load, of an arbitrary positive value P, travelling at the desired speed v. The resulting response (such as an acceleration or displacement time-history) is then scaled to the corresponding axle load and added to the total response, with a time offset related to the speed and the distance between axles.

As an example, a simple load model is considered, comprising four axle loads of 147.15 kN each, with a regular spacing of 3 m, running at a speed of 200 km/h. The overall effect is evaluated on the mid-span displacement of a 12 m simply supported bridge. Figure 1a depicts the displacement caused by a single load, while Fig. 1b illustrates the same response, multiplied and offset. The dashed line in Fig. 1c represents the sum of these effects and the bold line is the response of a separate calculation, on which the entire load model was set to run over the bridge model. The dotted line illustrates the difference between the two approaches, and its maximum absolute value is 3.6312×10^{-6} m.

The main advantage of implementing this approach is time reduction since the number of necessary time steps can be greatly reduced (the total running length corresponds only to the bridge model length, instead of the sum of the

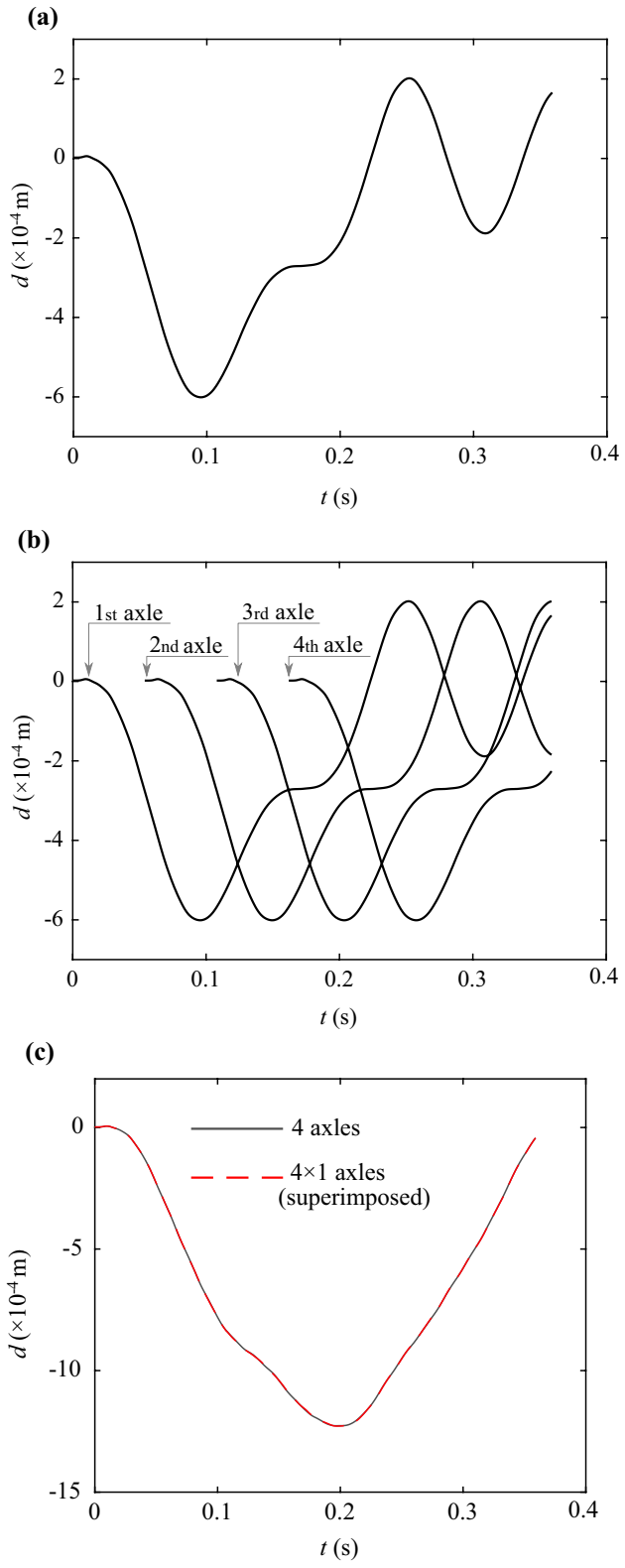

Fig. 1 Mid-span displacement of a single load and combined effect: **a** single load; **b** four axles; **c** combined response

bridge and train lengths). Also, by calculating the isolated response of an axle load, any load model response can be replicated by scaling and superimposing the known effects. The offset in the combination of actions can reproduce different axle spacings and the scaling can even be adjusted to different values in the same load model, e.g. where the loads of the power car are superior. Furthermore, if after the calculation of the effects for several load models on a bridge a new load model is required to be taken into consideration, there is no need for additional dynamic analysis, since the dynamic equations only have to be accessed once per speed value in order to save the single axle response.

The limitations of this methodology have to do with the moving load analysis, limiting its applicability to scenarios where there are no nonlinear aspects, such as wheel–rail contact. This leaves out train-bridge interaction analysis and the evaluation of criteria related to contact forces or car body acceleration. For the scope of the present work, this means that the discussed superposition method is applicable to the assessment of deck acceleration on ballasted tracks.

An example application is presented in Fig. 2, for the HSLM-A1 train. A single load $P = 170$ kN moves at a speed $v = 200$ km/h causing the mid-span displacement seen in Fig. 2a. On a commercially available 4-core computer, this operation took 149.751 s to complete, and the SLLS response, presented in Fig. 2b, was computed in 0.121 s. In comparison, the full load model of the HSLM-A1 that produces the response seen in the same figure took 34 min to be calculated.

2.3 Methodology application

The methodology proposed in this section addresses the questions listed in Sect. 1, having the goal of evaluating the HSLM-A coverage of trains made possible by Annex E of the EN 1991-2 and also of other trains whose properties fall outside those limits, to account for possible future vehicles. This methodology consists firstly in creating two sets of randomly generated load model configurations—"set *A*" abiding by the EN 1991-2 limits and "set *B*" employing wider limits—for each of the three train types, as detailed in Sect. 3.2 (sets A_a and B_a for articulated trains, A_c and B_c for conventional trains and A_r and B_r for regular trains). Afterwards, the dynamic signatures of all randomly generated trains and HSLM-A trains can be calculated, using Eq. (7). Then, to validate the conclusions, the dynamic response of all random trains is obtained for an example bridge. Since the SLLS approach is being used, only one dynamic analysis needs to be carried out since all different moving loads results can be derived from the single load

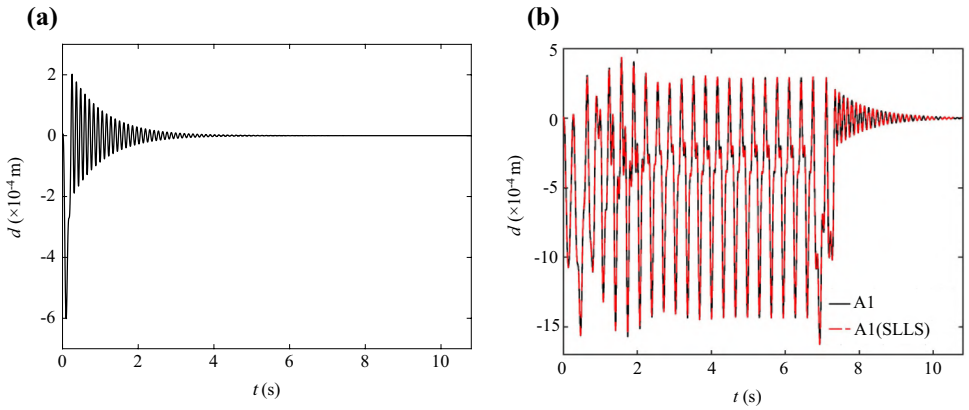

Fig. 2 Mid-span displacement of a single load and combined effect of HSLM-A1: **a** single load; **b** HSLM-A1

response. The same procedure is done for the 10 HSLM-A trains, thus allowing for a comparison to be established, using the maximum vertical deck acceleration as a metric. In this work, the selected example is the Canelas bridge (presented in Sect. 3.1), the sample size for the randomly generated sets is 100,000, the variable distribution is uniform and the speed range is from 140 to 420 km/h, with 10 km/h intervals (assuming a maximum line speed of 350 km/h, the EN 1991-2 defines the maximum design speed as 1.2 times that value, which gives $1.2 \times 350 = 420$). The samples for the random variables (D, d_{BA} d_{BS}, e_C, D_{IC} and D_L) are generated using a random number suited for uniform distributions, scaled to the limits detailed in Sect. 3.2.

A representative diagram of this methodology is presented in Fig. 3. The single load dynamic response is computed with a custom-built moving loads analysis application using [22].

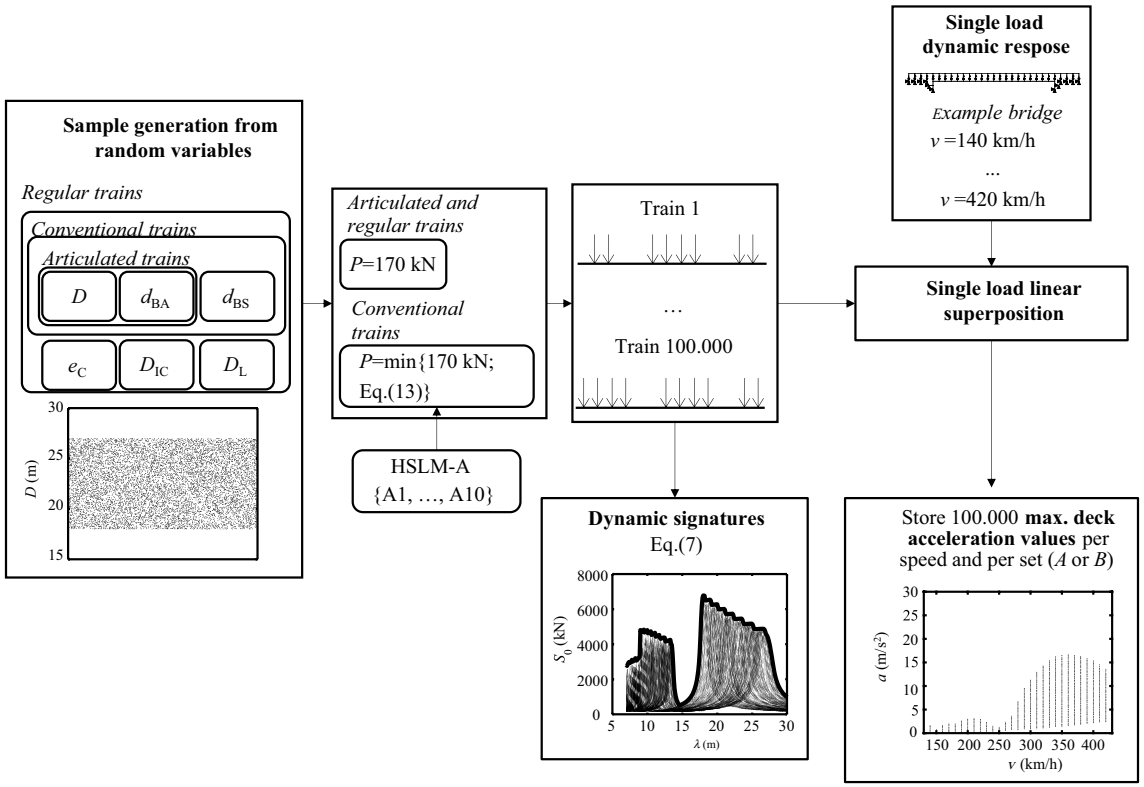

Fig. 3 Overview of the methodology to assess the HSLM limits of validity

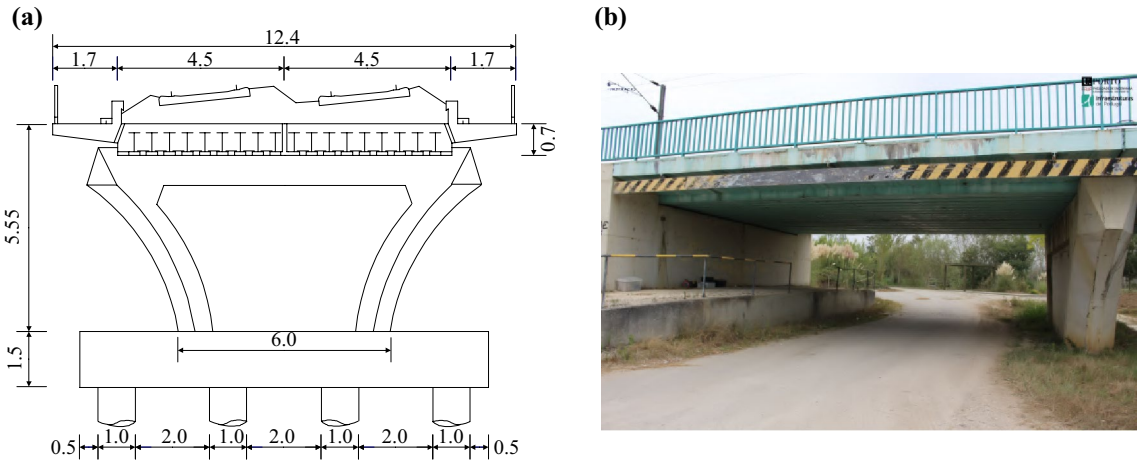

Fig. 4 Canelas bridge (unit: m): **a** cross section (adapted from [24]); **b** view of the first span

Table 1 Material and geometrical properties of the finite element model

Property name	Symbol	Value	Unit
Reinforced concrete density	γ_C	2.5	t/m^3
Concrete elasticity modulus	E_C	36.1	GPa
Slab thickness	t_{slab}	0.7	m
Slab width	b_{slab}	4.475	m
Area of the steel profiles	A_s	0.01975	m^2
Structural damping	ξ	2%	-
Ballast density	γ_b	1.8	t/m^3
Ballast elasticity modulus	E_b	120	MPa
Ballast height	h_b	450	mm
Load distribution angle	α	25	°
Sleeper mass	m_s	272.5	kg
Rail pad stiffness	k_p	350	kN/mm
Track shear stiffness	k_l	2×10^4	kN/m/m
Neoprene shear modulus	G_n	0.975	MPa
Steel elasticity modulus	E_S	210	GPa
Permanent loads	m_p	1.4	ton/m
Width of the sleeper underside	l_b	0.3	m
Half sleeper effective support	l_e	0.95	m
Sleeper spacing	l_s	0.6	m

3 Numerical modelling

3.1 Case study railway bridge

An existing bridge was selected as a case study. The Canelas bridge (Fig. 4) (built in 1996 on the Portuguese Railway Network's Northern Line) was chosen, given the already available information, regarding both experimental [23, 24] and numerical studies [25]. This filler beam structure comprises 6 simply supported 12 m spans, each formed by 2 independent decks constituted of concrete slabs directly cast on 9 embedded rolled steel profiles (HEB500). Each deck carries a ballasted track with UIC60 rails and is supported by a set of neoprene bearings.

To evaluate vertical deck acceleration, a 2D model of a single deck has been developed using [26] Parametric Design language, which allows the employment of several element types, specifically:

- COMBIN14: spring-dashpot elements, used in the track (for shear stiffness and for the separate representation of the ballast and rail pads stiffness) and in the bearing supports (in the vertical and horizontal directions, accounting for their flexibility).
- MASS21: mass point elements, used for the localized mass of the sleepers.
- BEAM3: beam elements, used to represent the rails and the deck.

The material and geometrical properties used in the model are listed in Table 1. In the model, the structural damping value is used to set Rayleigh factors (using the frequencies of the first and second vertical vibration modes) and the vertical stiffness of the ballast layer K_b is calculated in order to incorporate load distribution effects as proposed by [27]

$$K_{\mathrm{b}} = \begin{cases} K_{\mathrm{b}} = \dfrac{2(l_{\mathrm{e}} - l_{\mathrm{b}})\tan\alpha}{\ln\left[\left(\dfrac{l_{\mathrm{e}}}{l_{\mathrm{b}}}\right)(l_{\mathrm{b}} + 2h_{\mathrm{b}}\tan\alpha)/(l_{\mathrm{e}} + 2h_{\mathrm{b}}\tan\alpha)\right]} & \text{if } h_{\mathrm{b}}\tan\alpha \le \dfrac{l_{\mathrm{s}}}{2} \\ K_{\mathrm{b}} = \dfrac{K_{\mathrm{b1}}K_{\mathrm{b2}}}{K_{\mathrm{b1}} + K_{\mathrm{b2}}} & \text{if } h_{\mathrm{b}}\tan\alpha > \dfrac{l_{\mathrm{s}}}{2} \end{cases}, \tag{8}$$

where

$$K_{\mathrm{b1}} = \frac{2(l_{\mathrm{e}} - l_{\mathrm{b}})\tan\alpha}{\ln\left[(l_{\mathrm{e}}l_{\mathrm{s}})/(l_{\mathrm{b}}(l_{\mathrm{e}} + l_{\mathrm{s}} - l_{\mathrm{b}}))\right]}E_{\mathrm{b}}, \tag{9}$$

and

$$K_{\mathrm{b2}} = \frac{l_{\mathrm{s}}(l_{\mathrm{s}} - l_{\mathrm{b}} + 2l_{\mathrm{e}} + 2h_{\mathrm{b}}\tan\alpha)\tan\alpha}{l_{\mathrm{b}} - l_{\mathrm{s}} + 2h_{\mathrm{b}}\tan\alpha}E_{\mathrm{b}}. \tag{10}$$

Furthermore, the effect of load degradation underneath the sleepers was found to have a negligible effect on the global response of the deck. The stiffness of the spring elements representing the supports in both the vertical $K_{\mathrm{s,v}}$ and horizontal $K_{\mathrm{s,h}}$ directions includes all nine bearings (each comprised of two neoprene layers of 0.25 m × 0.15 m × 0.004 m and four neoprene layers of 0.25 m × 0.15 m × 0.008 m) on each end of the deck, and it was calculated according to [28, 29],

$$K_{\mathrm{s,v}} = \frac{n_{\mathrm{b}}}{\sum_{i=1}^{n_{\mathrm{l}}} \dfrac{t_i^3}{3G_{\mathrm{n}}a^3bf_{\mathrm{l}}f_2}}, \tag{11}$$

$$K_{\mathrm{s,h}} = \frac{n_{\mathrm{b}}abG_{\mathrm{n}}}{\sum_{i=1}^{n_{\mathrm{l}}} t_i}, \tag{12}$$

where n_{b} is the number of bearings, n_{l} is the number of neoprene layers in each bearing, t_i is each of the layer thickness, a is the smaller dimension (0.15 m), b is the largest dimension (0.25 m), f_{l} is a form factor dependent on a and b, and f_2 is a factor for dynamic loading, which depends on G_{n}.

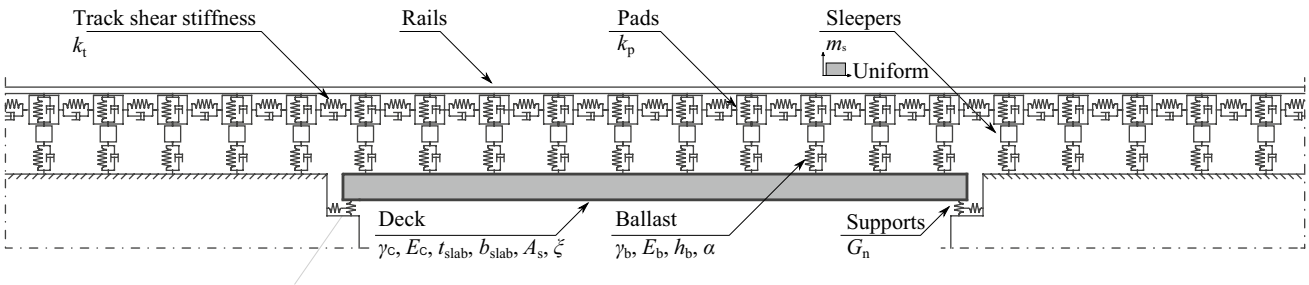

Fig. 5 Schematic representation of the filler beam bridge finite elements models and their random variables

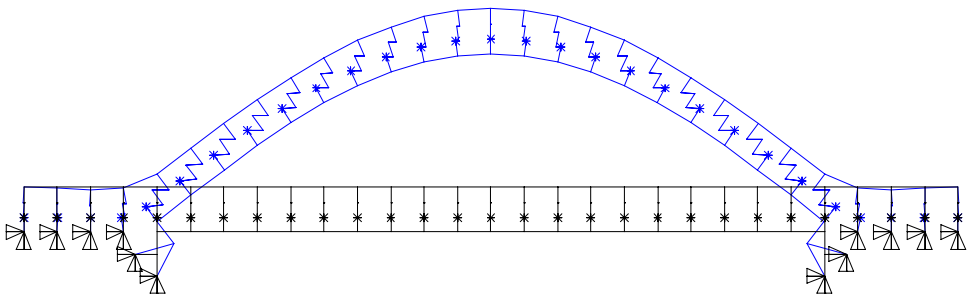

Fig. 6 Finite element model of the Canelas bridge (with the deformed shape of the first vertical bending mode)

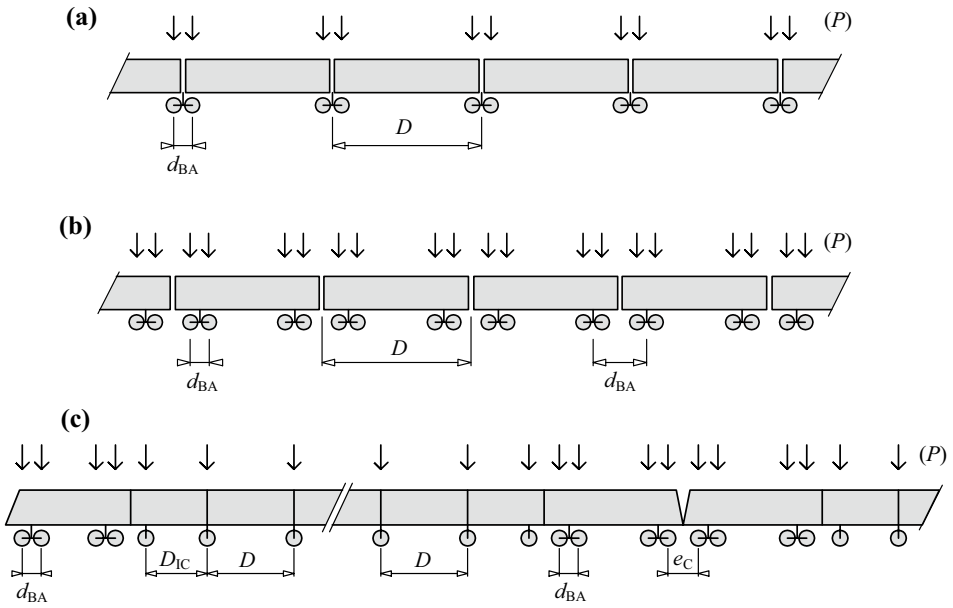

Fig. 7 Train type configurations (adapted from [9]): **a** articulated train; **b** conventional train; **c** regular train

Table 2 Random variables—articulated trains

Variable	Set A_a		Set B_a	
	Minimum (m)	Maximum (m)	Minimum (m)	Maximum (m)
D	18	27	15	30
d_{BA}	2.5	3.5	2	4

Table 3 Random variables—conventional trains

Variable	Set A_c		Set B_c	
	Minimum (m)	Maximum (m)	Minimum (m)	Maximum (m)
D	18	27	15	30
d_{BA}	2.5	3.5	2	4
d_{BS}	5.5	8.5	5.5	8.5

Figure 5 shows a schematic representation of the finite element model, which is shown in Fig. 6, alongside the deformed shape of the first vertical bending mode, corresponding to an eigenfrequency of 8.60 Hz (which is in the proximity of the 8.70 Hz experimentally assessed by Ref. [23]) In the figure, it can be seen that two additional track segments of 2.3 m were added on both sides of the deck. These extensions serve the purpose of providing a transition space where the moving loads can begin crossing the deck without being subjected to an abrupt change in track stiffness.

Table 4 Random variables—regular trains

Variable	Set A_r		Set B_r	
	Minimum (m)	Maximum (m)	Minimum (m)	Maximum (m)
D	10	14	8	16
d_{BA}	2.5	3.5	2	4
D_{IC}	8	11	6	13
e_C	7	10	5	12
d_{BS}	5.5	8.5	5.5	8.5
D_L	15.5	18.5	15.5	18.5

3.2 Load model configuration

Annex E of the EN 1991-2 lists the HSLM-A's limits of validity, concerning articulated, conventional and regular trains. Figure 7 illustrates the three types of trains, where:

- P is the individual axle load;
- D is the coach length or distance between regularly repeating axles;
- d_{BA} is the distance between axles of the same bogie;
- d_{BS} is the distance between the centres of adjacent vehicle bogies;
- D_{IC} is the intermediate coach length (regular trains);
- e_c is the distance between consecutive axles on the coupling of two trainsets (regular trains).

P is limited to 170 kN or, for conventional trains, the lesser of 170 kN and the value that comes from Eq. (13), where

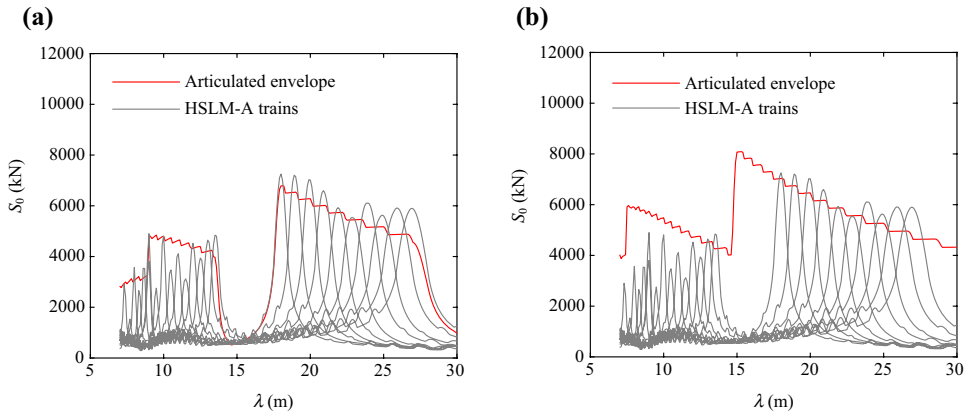

Fig. 8 Dynamic signatures of articulated trains: **a** set A_a; **b** set B_a

P_{HSLMA}, d_{HSLMA} and D_{HSLMA} are the corresponding properties of the Universal Trains. This can be a single Universal Train if D matches an existing D_{HSLMA} or two Universal trains otherwise, selecting the two whose D_{HSLMA} values are just greater and just lesser than D. D should be between 18 and 27 m for articulated and conventional trains or between 10 and 14 m for regular trains, while D_{BA} lies between 2.5 and 3.5 m.

While the norm lacks in providing limits for d_{BS}, it states that D/d_{BA} and $\left(d_{\mathrm{BS}} - d_{\mathrm{BA}}/d_{\mathrm{BA}}\right)$ should not approach integer values and that d_{BS} must be in accordance with Eq. (13). D_{IC} must be between 8 and 11 m and e_{C} between 7 and 10 m. In addition, there are also limits for total train weight (10000 kN), length (400 m) and unsprung axle mass (2 tonnes).

$$4P\cos\left(\frac{\pi d_{\mathrm{BS}}}{D}\right)\cos\left(\frac{\pi d_{\mathrm{BA}}}{D}\right) \leq 2P_{\mathrm{HSLMA}}\cos\left(\frac{\pi d_{\mathrm{HSLMA}}}{D_{\mathrm{HSLMA}}}\right). \tag{13}$$

For articulated trains, the sets of random variables are listed in Table 2, where set A_a contains the variables as defined in the norm and set B_a has the wider limits, intended to represent the influence of future (and existing) trains that do not necessarily respect the norm limits. The point load value P is set to its maximum allowed of 170 kN, since the highest value corresponds to the maximum acceleration registered.

The variables for conventional trains are presented in Table 3. As previously discussed, there are no set limits for variable d_{BS}, and for that reason, its values on set A_c (which stem from the real trains of types A, D and F on [7]) remain unaltered on set B_c. Since the maximum allowed value of P for conventional trains is the lesser of 170 kN and the value resulting from Eq. (13), all randomly generated samples must undergo that check.

Regarding regular trains, the random variables are itemized in Table 4. An additional variable D_{L} is here defined to represent the length of the first and last coaches of each trainset. Its limits are the same in both set A_r and set B_r due to the same reason considered for variable d_{BS} (which for regular trains represents the distance between the centremost bogies of the first and last coache and the closest axle of the intermediate coach). In both sets, P has a value of 170 kN.

4 Results discussion

Following the methodology described in Sect. 2.3, the obtained results are here presented—firstly concerning the dynamic signatures (calculated directly from the sampled distances), followed by the response of the case study bridge. For each type of train, the influence of the individual variables is evaluated by assessing selected samples from set B.

4.1 Preliminary analysis based on train signatures

Given that the case study bridge is a simply supported span, in order to study the HSLM-A the dynamic signatures that follow are presented for wavelengths starting at 7 m, as per the EN 1991-2. Figure 8 represents the envelope of articulated trains' signatures, for both sets, as the line in red. Each of the 10 light grey lines represents one of the HSLM-A universal trains. It can be seen that the load model provides good coverage of the complying articulated trains, particularly above wavelengths of 6 m, while the sampled set B_a yields higher spectra.

For conventional trains, the dynamic signatures represented in Fig. 9 also show a better coverage for set A_c than for set B_c. It appears to be, however, a lack of coverage in wavelengths up to 12 m, even for set A_c. This finding motivates

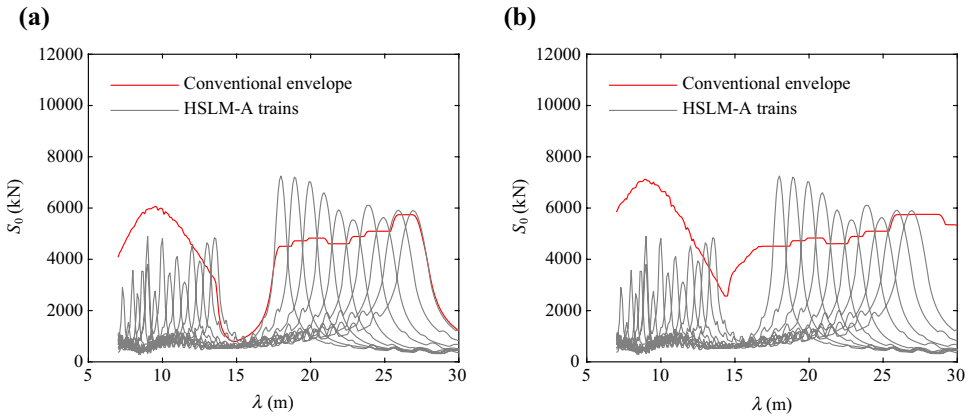

Fig. 9 Dynamic signatures of conventional trains: **a** set A_c; **b** set B_c

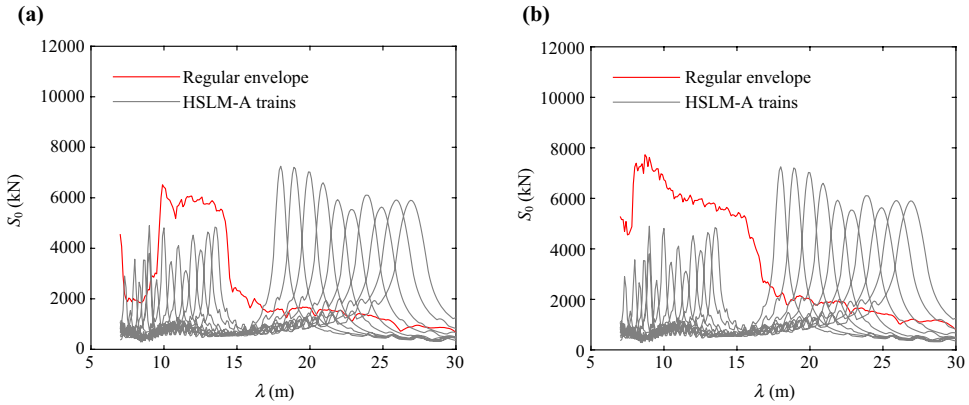

Fig. 10 Dynamic signatures of regular trains: **a** set A_r; **b** set $\mathbf{B}_r$

looking into the dynamic analyses to understand whether or not this is due to the influence of any of the variables.

As for regular trains, in Fig. 10, the shown dynamic signatures lead to a similar conclusion regarding the difference between sets A_r and B_r, particularly in the fact that even in set A_r lower wavelengths (up to 17 m) can lead to results above the HSLM-A's. On the other hand, the larger difference to the HSLM-A dynamic signatures in the 17–30 m range is noted, in comparison to the previously discussed articulated and conventional train types.

4.2 Numerical analysis

The following results represent the entirety of stochastic dynamic analyses performed on the case study bridges, with the same randomly generated train configurations that constitute sets A and B for the 3 types of trains. The goal is to validate the conclusions obtained from the signature analysis regarding the HSLM coverage and to better understand which variables contribute the most to the presence of extreme values. The present section reflects a total of 17.4 dynamic million analyses, i.e. the product of the sample size (100.000), number of speed values (29) and number of sets of random variables (6 sets: A_a, B_a, A_c, B_c, A_r, B_r).

4.2.1 Articulated trains

The results from the dynamic analyses regarding articulated trains are represented in Fig. 11, for both sets, where each dot represents the maximum vertical deck acceleration calculated for each sampled train. The line in full, which remains unaltered in both sets, is the envelope of the 10 HSLM-A universal train responses, as per the graph in Fig. 3. Observing the results, it can be seen that the sample set generated within the norm's limits is adequately covered by the HSLM, apart from a few outliers (which is in accordance with the findings by Museros et al. [21]). As expected, the resulting values from set B_a are not covered by the load model, especially in higher velocities. This finding is unfavourable towards the first question listed in Sect. 1, although it is stated that this matter is not the main focus of the present study.

To better understand the independent influence of each variable, Figs. 12 and 13 present selections of results from set B_a, alternately highlighting a variable's influence when

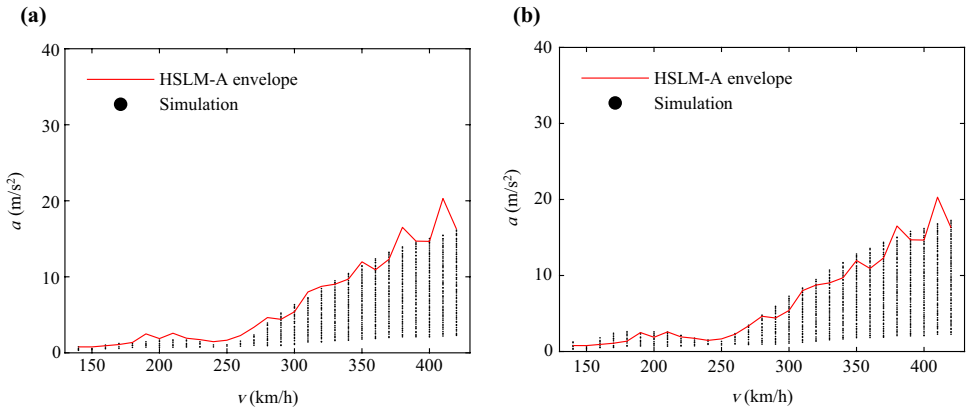

Fig. 11 Dynamic response of articulated trains: **a** set A_a; **b** set B_a

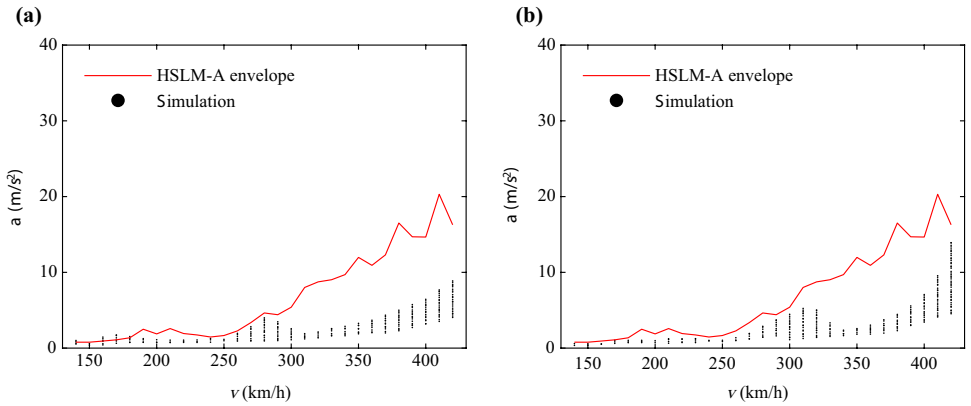

Fig. 12 Articulated trains—selected results from set B_a highlighting variable D: **a** 15 m ≤ D ≤ 18 m, 2.5 m ≤ d_{BA} ≤ 3.5 m, **b** 27 m ≤ D ≤ 30 m; 2.5 m ≤ d_{BA} ≤ 3.5 m

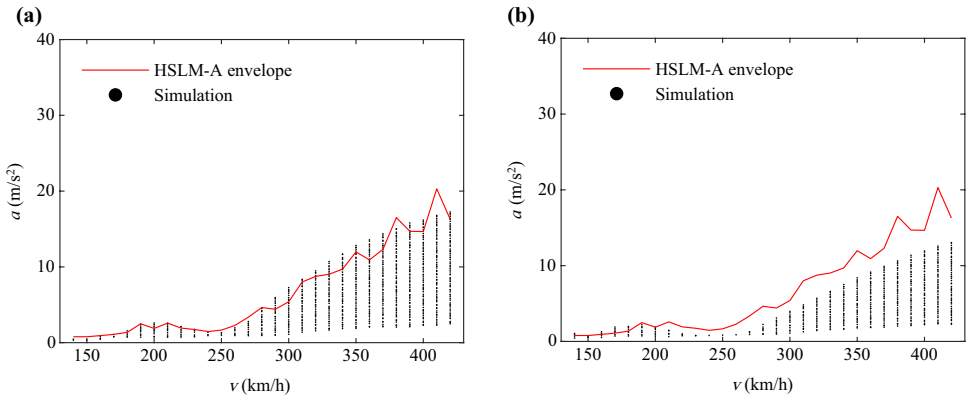

Fig. 13 Articulated trains—selected results from set B_a highlighting variable d_{BA}. **a** 18 m ≤ D ≤ 27 m, 2 m ≤ d_{BA} ≤ 2.5 m; **b** 18 m ≤ D ≤ 27 m, 3.5 m ≤ d_{BA} ≤ 4 m

it is taken above or below the stated limits of validity while selecting the complying values for the other variables. From Fig. 12, it can be seen that there is a similar contribution from simulated trains whose coach length is inferior to the limit and due to those that are above it.

As for the distance between axles (Fig. 13), while its lower values lead to higher results, its consequences are not as notorious. In fact, as D decreases, resonant effects become more noticeable in the bridge taken as the example in this study.

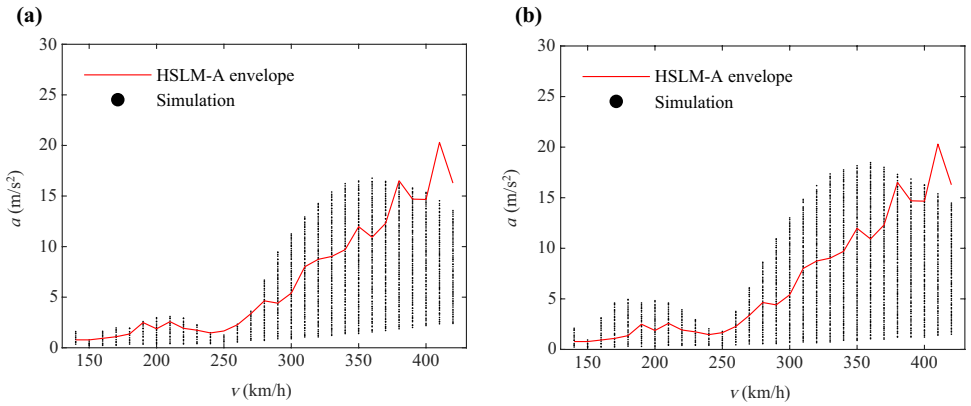

Fig. 14 Dynamic response of conventional trains: **a** set A_c; **b** set B_c

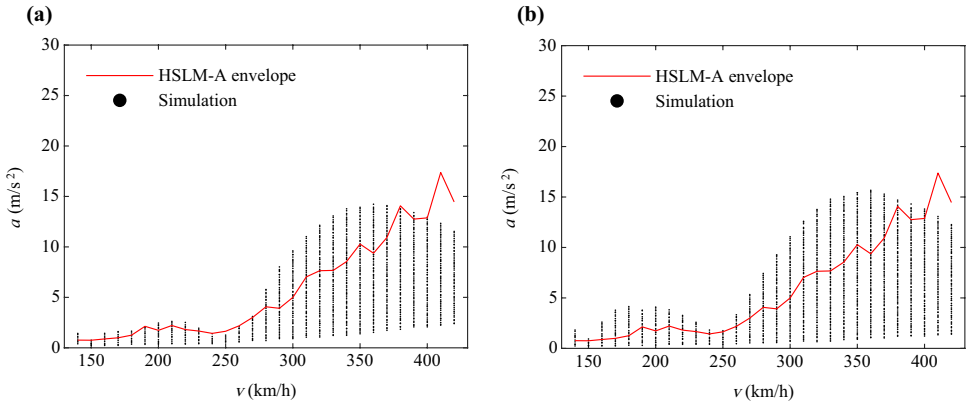

Fig. 15 Dynamic response of conventional trains (with additional damping): **a** set A_c; **b** set B_c

4.2.2 Conventional trains

The results of the dynamic analyses with conventional trains are shown in Fig. 14. In it, it is noted that even set A_c, which is in accordance with the normative limits, hosts load model configurations that cause dynamic effects greater than those produced by the HSLM-A universal trains. The lack of coverage discussed with the dynamic signatures is once more present in a corresponding range of wavelengths. In fact, considering that the frequency of the first vertical bending mode for the bridge is 8.60 Hz, the wavelength range corresponding to the 280 to 370 km/h speed range is 9.04 to 11.95 m.

Sets A_c and B_c were selected to infer the effects of including additional damping in the dynamic analyses. For that, a new single load was generated from the FE model of the Canelas bridge, considering a total structural damping ξ_{total} of

$$\begin{aligned}\xi_{total} &= \xi + \Delta\xi = 2\% + \frac{0.0187L - 0.00064L^2}{1 - 0.0441L - 0.0044L^2 + 0.000255L^3}\% \\ &= 2\% + 0.476\% = 2.476\%.\end{aligned} \tag{14}$$

The results of the dynamic analyses, as well as the HSLM envelopes generated with additional damping, are shown in Fig. 15. Both the simulations distribution and the envelopes present themselves as scaled-down versions of the responses without additional damping of Fig. 14. The relation between the randomly generated train load models and the HSLM is maintained, and the issue raised before (i.e. load configurations in set A_c that surpass the HSLM-A envelope) is still observable.

As before, it can be seen that the exceedingly higher values on the highest speeds correspond to the lowest values of D (Fig. 16). On the other hand, it is the higher values of d_{BA} that result in lower acceleration peaks (Fig. 17). In fact, the only scenario where the outlying values between 280 and 370 km/h tend to disappear is the scenario considering d_{BA} values above the allowed limit. To better understand this phenomenon, Fig. 18 shows the distribution of variable d_{BS} from simulations whose dynamic response is superior to that of the HSLM, for two example speed values within the 280–370 km/h range. It is visible that the outlying simulated trains correspond to increasingly higher values

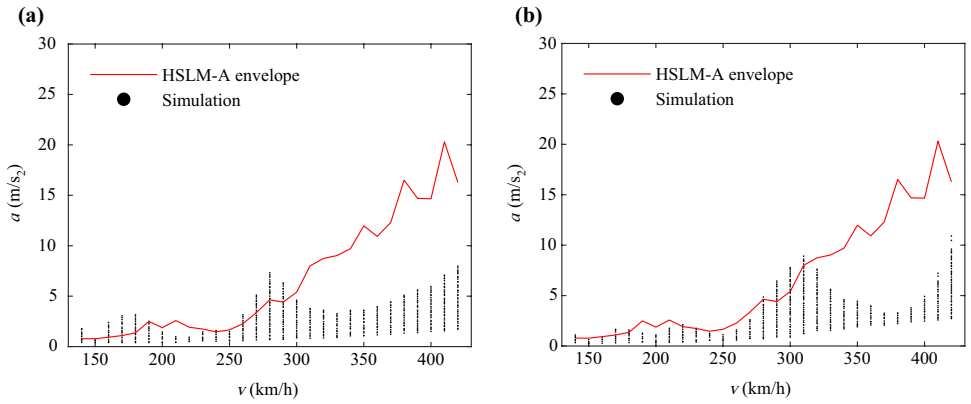

Fig. 16 Conventional trains—selected results from set B_c highlighting variable D: **a** 15 m ≤ D ≤ 18 m, 2.5 m ≤ d_{BA} ≤ 3.5 m; **b** 27 m ≤ D ≤ 30 m, 2.5 m ≤ d_{BA} ≤ 3.5 m

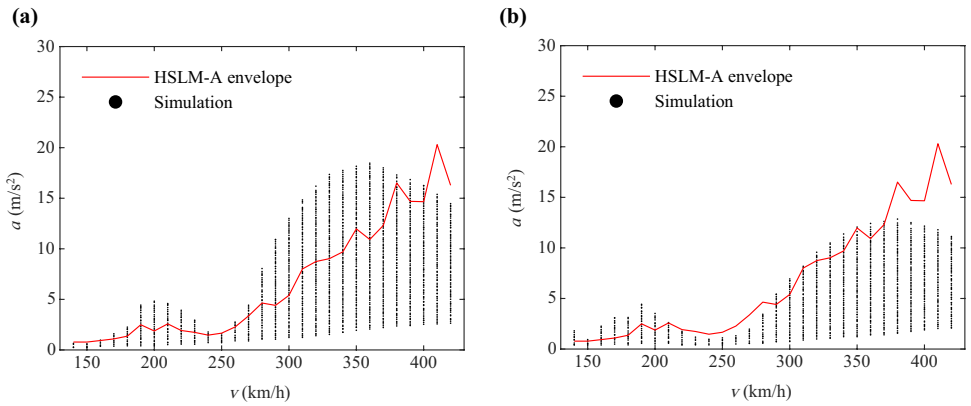

Fig. 17 Conventional trains—selected results from set B_c highlighting variable d_{BA}: **a** 18 m ≤ D ≤ 27 m, 2 m ≤ d_{BA} ≤ 2.5 m; **b** 18 m ≤ D ≤ 27 m, 3.5 m ≤ d_{BA} ≤ 4 m

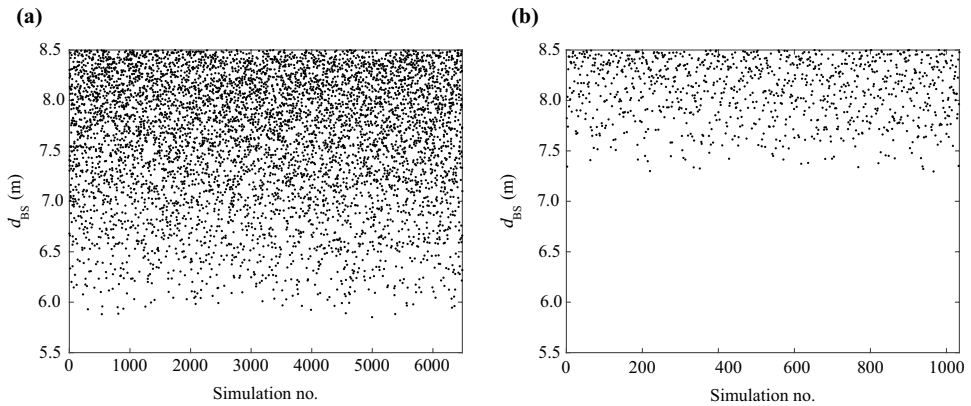

Fig. 18 Dynamic response of conventional trains—distribution of variable d_{BS} on simulations above the HSLM envelope, from set B_c: **a** 300 km/h; **b** 350 km/h

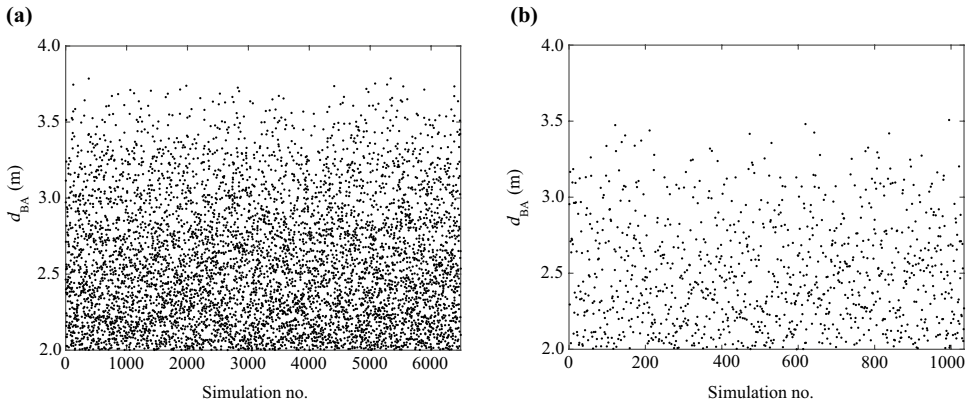

Fig. 19 Dynamic response of conventional trains—distribution of variable d_{BA} on simulations above the HSLM envelope, from set B_c: **a** 300 km/h; **b** 350 km/h

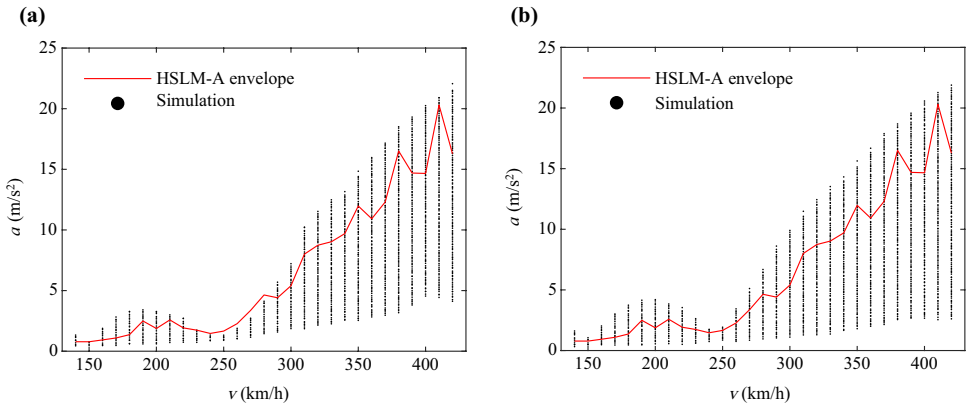

Fig. 20 Dynamic response of regular trains: **a** set A_r; **b** set B_r

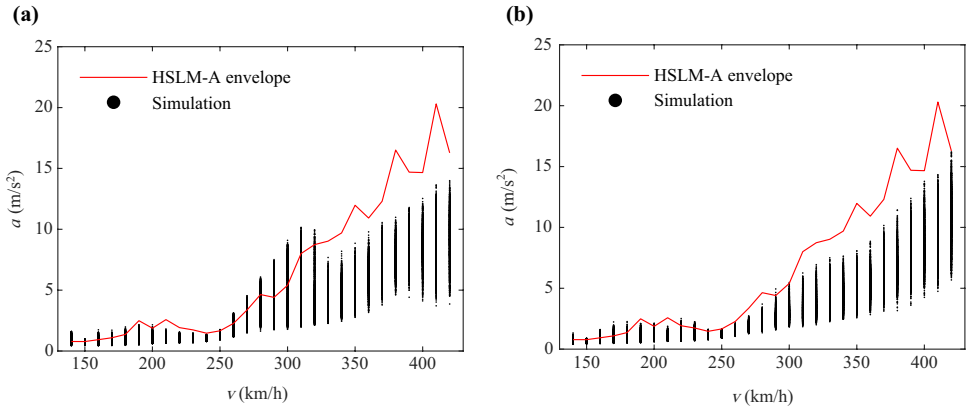

Fig. 21 Regular trains—selected results from set B_r highlighting variable D: **a** 8 m ≤ D ≤ 10 m, 2.5 m ≤ d_{BA} ≤ 3.5 m, 8 m ≤ D_{IC} ≤ 11 m, 7 m ≤ e_C ≤ 10 m; **b** 14 m ≤ D ≤ 16 m, 2.5 m ≤ d_{BA} ≤ 3.5 m, 8 m ≤ D_{IC} ≤ 11 m,7 m ≤ e_C ≤ 10 m

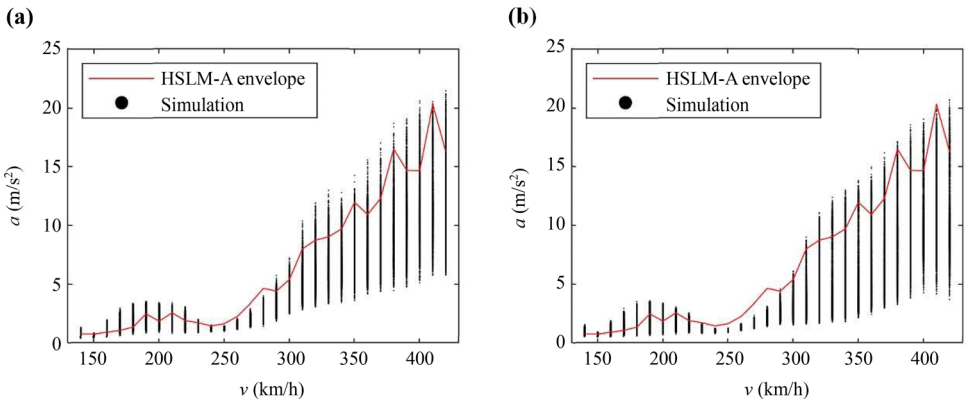

Fig. 22 Regular trains—selected results from set B_r highlighting variable d_{BA}: **a** 10 m ≤ D ≤ 14 m, 2 m ≤ d_{BA} ≤ 2.5 m, 8 m ≤ D_{IC} ≤ 11 m, 7 m ≤ e_C ≤ 10 m; **b** 10 m ≤ D ≤ 14 m, 3.5 m ≤ d_{BA} ≤ 4 m, 8 m ≤ D_{IC} ≤ 11 m, 7 m ≤ e_C ≤ 10 m

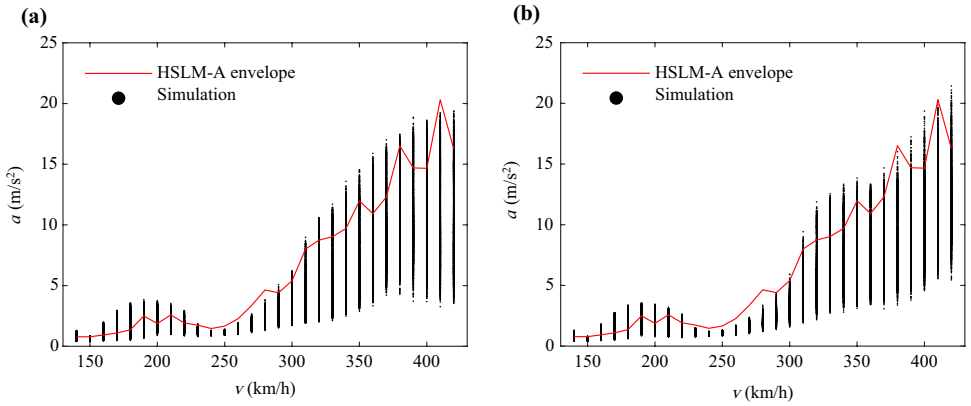

Fig. 23 Regular trains—selected results from B_r highlighting variable D_{IC}: **a** 10 m ≤ D ≤ 14 m, 2.5 m ≤ d_{BA} ≤ 3.5 m, 6 m ≤ D_{IC} ≤ 8 m, 7 m ≤ e_C ≤ 10 m; **b** 10 m ≤ D ≤ 14 m, 2.5 m ≤ d_{BA} ≤ 3.5 m, 11 m ≤ D_{IC} ≤ 13 m, 7 m ≤ e_C ≤ 10 m

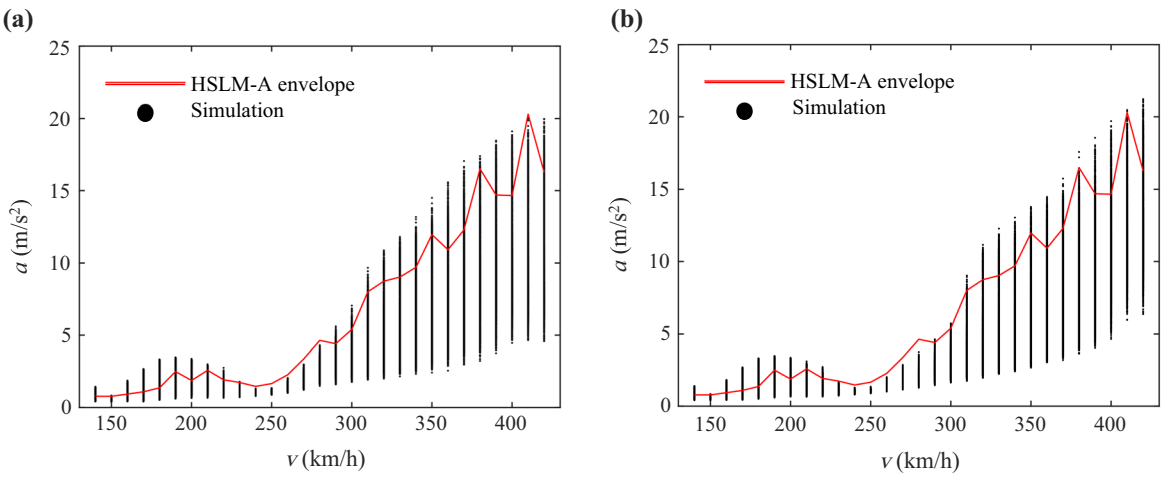

Fig. 24 Regular trains—selected results from set B_r highlighting variable e_C: **a** 10 m ≤ D ≤ 14 m, 2.5 m ≤ d_{BA} ≤ 3.5 m, 8 m ≤ D_{IC} ≤ 11 m, 5 m ≤ e_C ≤ 7 m; **b** 10 m ≤ D ≤ 14 m, 2.5 m ≤ d_{BA} ≤ 3.5 m, 8 m ≤ D_{IC} ≤ 11 m, 10 m ≤ e_C ≤ 12 m

of this variable. This observation underlines the pertinence of the third question listed in Sect. 1 since the Eurocode could be clearer in defining limits for this distance. When looking at the distribution of variable d_{BA} from the same samples (illustrated in Fig. 19), a concentration on lower values appears. Therefore, it can be concluded that the most aggressive scenarios correspond to higher d_{BS} and lower d_{BA}. Indeed, as d_{BS} increases (approaching D), the regularity of the moving loads grows, contributing to dynamic effects. As for d_{BA}, as it decreases, the effect of the pair of moving loads approaches that of a single double-load.

4.2.3 Regular trains

The dynamic responses of sets A_r and B_r for regular trains are presented in Fig. 20. While both sets contain train load configurations that result in acceleration values above the HSLM-A's, set A_r distributions tend to follow the trend of the envelope more closely throughout the entire speed range. From the individual variable influence, in this case there is some variability caused by D (Fig. 21), while variable d_{BA} (Fig. 22) is the less influential. The same can be observed for the D_{IC} (Fig. 23) and e_C (Fig. 24) variables, although it should be highlighted that the former only controls four load distances and the latter a single one.

5 Conclusion

The conclusions of this study are summarized according to the questions listed in Sect. 1 as follows:

1. With the extended limits considered in this study, it can be said that the HSLM-A is partially suited to represent some future trains, given the similarity in the results for both sets A and B on speeds up to 400 km/h (of the selected example bridge), or wavelengths excluding the 15–17 m range. Nevertheless, this should not be thought of as a lack of the load model readiness but more of as an indicator of the need for future-proofing.
2. The 10 HSLM-A universal trains do not cover the dynamic effects of some theoretical train load models that can be constructed abiding by the EN 1991-2 limits of validity. This happens in some limit cases of articulated trains, but it is most prevalent in conventional and regular trains, although it should be noted that the last two train types are lacking in the definition of some variables. In conventional trains, there is a relation between the non-complying trains and the increasing distance between centres of adjacent vehicle's bogies—as this variable increases, the effect of consecutive bogies acts progressively more as individual loads and less as pairs, which in turn leads to higher vertical acceleration levels, due to the contribution that the loads repetition has to resonant effects.
3. The definition of variable d_{BS} in the norm is insufficient and this constitutes an obstacle to the evaluation of the HSLM's limits of validity, which is made more apparent when this variable's importance is noted. There is also a challenge in defining the two distances, not mentioned in the norm, necessary to characterize regular trains.

It is therefore understood that there is some margin for improvement in Annex E of the EN 1991-2, not only by providing better definitions of some distances but also by adjusting the HSLM-A's universal trains. In this regard, future work should focus on parametric studies for the definition of the proposed load models, including equivalent train–track–bridge interaction models with replication of the HSLM's effects. The methodology applied in this work to assess the dynamic response of the case study bridge and the efficiency of the HSLM in covering the effects of different trains can be utilized and replicated for a number of different high-speed railway bridges. The present study draws the conclusion that there are issues with the current load model from the analysis of a case study filler beam bridge, and therefore, a future publication should include integral portal frames, composite concrete-steel structures and metallic truss bridges, in different spans lengths. In addition, the probability of trains crossing on a bridge and the effects of such phenomenon are also considered for future work.

Acknowledgements This work was financially supported by the Portuguese Foundation for Science and Technology (FCT) through the PhD scholarship PD/BD/143007/2018. The authors would like also to acknowledge the financial support of the projects IN2TRACK2—Research into enhanced track and switch and crossing system 2 and IN2TRACK3—Research into optimised and future railway infrastructure funded by European funds through the H2020 (SHIFT2RAIL Innovation Programme) and of the Base Funding—UIDB/04708/2020 of the CONSTRUCT—Instituto de I &D em Estruturas e Construções—funded by national funds through the FCT/MCTES (PIDDAC).

References

1. Zhang N, Zhou Z, Wu Z (2022) Safety evaluation of a vehicle-bridge interaction system using the pseudo-excitation method. Railw Eng Sci 30(1):41–56
2. Gong W, Zhu ZY, Liu R et al (2020) Running safety assessment of a train traversing a three-tower cable-stayed bridge under spatially varying ground motion. Railw Eng Sci 28(2):184–198
3. Montenegro PA, Carvalho H, Ribeiro D et al (2021) Assessment of train running safety on bridges: a literature review. Eng Struct 241:112425
4. Commité European de Normalisation (2005) Eurocode 0—Basis of structural design—Annex A2: applications for bridges (normative). Brussels
5. Zacher M, Baeßler M (2008) Dynamic behaviour of ballast on railway bridges. In: Dynamics of high-speed railway bridges. CRC Press, London
6. European Rail Research Institute (1999) Rail bridges for speeds > 200 km/h: Confirmation of values against experimental data, ERRI D 214/RP 8. Utrecht
7. European Rail Research Institute (1999) Rail bridges for speeds > 200 km/h: Final report, ERRI D 214/RP 9. Utrecht
8. European Commission (2014) Commission Regulation (EU) No 1299/2014 of 18 November 2014 on the technical specifications for interoperability relating to the 'infrastructure' subsystem of the rail system in the European Union Text with EEA relevance. http://data.europa.eu/eli/reg/2014/1299/oj/eng
9. Commité European de Normalisation (2003) Eurocode 1—part 2: Actions on structures—traffic load on bridges. Brussels
10. European Rail Research Institute (1999) Rail bridges for speeds > 200 km/h: Calculations for bridges with simply supported beams during the passage of a train ERRI D 214/RP 6. Utrecht
11. Vestroni F, Vidoli S (2007) Closed-form solutions for the structural response to train loads. J Sound Vib 303(3):691–706
12. Matsuoka K, Collina A, Somaschini C et al (2019) Influence of local deck vibrations on the evaluation of the maximum acceleration of a steel-concrete composite bridge for a high-speed railway. Eng Struct 200:109736
13. Auersch L (2021) Resonances of railway bridges analysed in frequency domain by the modal-force-excitation, bridge-transfer and axle-sequence spectra. Eng Struct 249:113282
14. Marvillet D, Tartary JP (2003) Bridges, high speed and dynamic calculation - short version. In: IABSE Symposium: Structures for High-Speed Railway Transportation, Antwerp, pp 80–81
15. Bernhard G, Josef F (2021) A redesigned approach to the additional damping method in the dynamic analysis of simply supported railway bridges. Eng Struct 241:112415
16. Reiterer M, Firus A, Vorwagner A et al (2021) Railway bridge dynamics: Development of a new high-speed train load model for dynamic analyses of train crossing. In: IABSE Congress Ghent 2021—Structural Engineering for Future Societal Needs, Ghent, pp 1633–1642
17. Andersson A, Allahvirdizadeh R, Albright A et al (2021) Report No. D5.6–Performed high-speed low-cost bridges I2T3 demonstrators. H2020-Sift2Rail-In2Track3 project: Research into optimised and future railway infrastructure (S2R-CFM-IP3-01-2020 Innovation Action). Tunnel and Bridge I2T2 Report-High speed low cost bridges-D5.2.5. Porto, Stockholm and Valencia
18. Reiterer M, Kohl AM, Vorwagner A et al (2022) Development of a new high-speed load model and validation on existing railway bridges. In: The 5th International Conference on Railway Technology: Research, Development and Maintenance, Montpellier
19. Vorwagner A, Kwapisz M, Flesch R et al (2021) FEM based approach for development of a new high-speed load model for railway bridges. In: IABSE Congress, Ghent 2021—Structural Engineering for Future Societal Needs, Ghent, pp 1614–1622
20. Harald U, Schörghofer DA, Taras A (2017) Critical bridges in high-speed railway lines: systematic identification for specific trains. In: 8th European Conference on Steel and Composite Structures (Eurosteel 2017), Copenhagen, pp 1427–1436
21. Museros P, Andersson A, Martí V et al (2021) Dynamic behaviour of bridges under critical articulated trains: signature and bogie factor applied to the review of some regulations included in EN 1991–2. Proc Instit Mech Eng Part F J Rail Rap Transit 235(5):655–675
22. MATLAB ® (2018) version 9.4.0.813654 (R2018a). The Mathworks, Inc., Natick
23. Bonifácio C, Ribeiro D, Calçada R et al (2014) Calibration and validation of the numerical model of a short-span railway bridge based on dynamic tests. In: Proceedings of the 9th International Conference on Structural Dynamics, Porto, pp 1315–1321
24. Pimentel R, Barbosa C, Costa N et al (2007) Characterization of railway traffic and its effects on a short span bridge by sing a hybrid fibre optic/electrical measurement system. In: Third European Workshop on Optical Fibre Sensors, Naples, pp 66193Y. International Society for Optics and Photonics
25. Rocha JM, Abel HA, Rui C (2016) Probabilistic assessment of the train running safety on a short-span high-speed railway bridge. Struct Infrastruct Eng 12(1):78–92
26. ANSYS®, (2018) Release 19.2. ANSYS Inc., Canonsburg, Pennsylvania
27. Zhai W, Wang K, Lin J (2004) Modelling and experiment of railway ballast vibrations. J Sound Vib 270(4):673–683
28. Manterola J (2006) Puentes: apuntes para su diseño, cálculo y construcción. Colegio de Ingenieros de Caminos, Canales y Puertos.
29. Rocha J (2015) Probabilistic methodologies for the safety assessment of short span railway bridges for high-speed traffic. Dissertation, Faculdade de Engenharia da Universidade do Porto